Journal of Inorganic and General Chemistry
ZAAC
Zeitschrift für anorganische und allgemeine Chemie
DOI: 10.1002/zaac.201800297
ARTICLE

Synthesis and Molecular Structure of *trans*-[$RhCl_2(tBu_2PPh)_2$]: a Rare Example of a Mononuclear Rhodium(II) Complex

Hans-Christian Böttcher,*[a] Peter Klüfers,[a] Thomas Mies,[a] and Peter Mayer[a]

Dedicated to Professor Peter Comba on the Occasion of His 65th Birthday

Abstract. During the reaction of [{Rh(μ-Cl)(coe)$_2$}$_2$] (**1**) (coe = *cis*-cyclooctene) with the tertiary phosphane tBu_2PPh in a nitrogen atmosphere the square planar rhodium(II) complex *trans*-[$RhCl_2(tBu_2PPh)_2$] (**2**) was identified as a side product in moderate yield. **2** was synthesized in a defined manner in higher yields using a known procedure starting from [{Rh(μ-Cl)(coe)$_2$}$_2$], tBu_2PPh (molar ratio Rh:P of 1:2), and *N*-chlorosuccinimide as the oxidizing agent in THF at room temperature. The molecular structure of **2** was determined by X-ray crystallography. Additionally, to further confirm the molecular structure of *trans*-[$RhCl_2(tBu_2PPh)_2$], extensive DFT calculations were undertaken, which gave further evidence for its molecular structure. In contrast to the remarkable stability of **2** in the solid state, the investigation of solutions of this compound afforded hints at a dynamic equilibrium, which renders more difficult the collection of adequate NMR spectroscopic data for the title complex.

Introduction

Recently we reported investigations on the reaction of [{Rh(μ-Cl)(coe)$_2$}$_2$] (**1**) (coe = *cis*-cyclooctene) with the secondary phosphane tBu_2PH in different solvents using various molar ratios of reactants.[1] Operating in heptane (molar ratio Rh:P of 1:2) afforded [{Rh(μ-Cl)(tBu_2PH)$_2$}$_2$] in nearly quantitative yield and the molecular structure of the latter in the solid was confirmed by X-ray diffraction.

In this context we were interested in the analogous reaction using the tertiary phosphane tBu_2PPh to obtain the related complex [{Rh(μ-Cl)(tBu_2PPh)$_2$}$_2$] by the same way. Unfortunately, till now, we were unable to grow suitable crystals of the latter for an X-ray diffraction study to confirm its molecular structure. During the chosen synthetic procedure and by subsequent crystallization attempts we obtained by accident a side product, which crystallized as well-shaped dark red crystals. An X-ray diffraction study revealed this species to be the Rh^{II} complex *trans*-[$RhCl_2(tBu_2PPh)_2$]. This compound represents one of the rare mononuclear rhodium(II) complexes, which had been described in the literature to date. Thus we focused our efforts on a systematical preparation of this species. A literature study showed that there have been only a few structural reports on complexes with the composition *trans*-[$RhCl_2(PR_3)_2$].[2] While rhodium(II) complexes have been found often as dinuclear species with bridging ligands and metal–metal bonds, some types of ligands (e.g., porphyrines, pincer ligands, pyridinophanes) were used to stabilize mononuclear Rh^{II} and, partially, Ir^{II} compounds.[3]

The reaction of [{Rh(μ-Cl)(coe)$_2$}$_2$] (**1**) with tBu_2PPh (molar ratio Rh:P of 1:2) in heptane as the solvent in a *nitrogen* atmosphere afforded – in contrast to the reaction of **1** with tBu_2PH – a mixture of compounds containing [{Rh(μ-Cl)(tBu_2PPh)$_2$}$_2$] as the main product beside considerable amounts of the dinitrogen complex *trans*-[$RhCl(N_2)(tBu_2PPh)_2$]. The latter compound was isolated as suitable crystals for an X-ray diffraction study. Unfortunately, because of disorder phenomena concerning the positions of the chlorido and the dinitrogen ligand in crystals of the latter, these data are only preliminary. Other authors reported the same disorder phenomenon in crystals of *trans*-[$RhCl(N_2)(PiPr_3)_2$].[4] Now we found that the reaction of **1** with tBu_2PPh in an *argon* atmosphere yielded [{Rh(μ-Cl)(tBu_2PPh)$_2$}$_2$] as the sole product.

During attempts to crystallize the latter compound from dichloromethane solutions in a nitrogen atmosphere we obtained a crop of red crystals suitable for X-ray work. A first structure solution and refinement (wR_2 = 0.1141) showed that *trans*-[$RhCl_2(tBu_2PPh)_2$] (**2**) was obtained as a product resulting from an unknown side reaction. Such mononuclear paramagnetic Rh^{II} compounds have been known for many years and were isolated from reactions of rhodium(III) chloride with phosphanes or were observed as impurities during reactions of chloridorhodium(I) complexes bearing olefin ligands.[5,6] X-ray analyses on this type of complex are scarce. Thus, the crystal and molecular structure of *trans*-[$RhCl_2(PPh_3)_2$] was reported.[6] This species was discussed earlier as a paramagnetic impurity during the synthesis of Wilkinson's catalyst [$RhCl(PPh_3)_3$]. Unfortunately, the latter structure analysis was not correct and other authors examined some times later the structure analysis in detail. They recognized this

* Prof. Dr. H.-C. Böttcher
Fax: +49-89-2180-77407
E-Mail: hans.boettcher@cup.uni-muenchen.de
[a] Department Chemie
Ludwig-Maximilians-Universität
Butenandtstr. 5–13 (D)
81377 München, Germany
Supporting information for this article is available on the WWW under **http://dx.doi.org/10.1002/zaac.201800297** or from the author.

species as *trans*-[RhCl(CO)(PPh_3)$_2$] crystallizing orthorhombically as yellow crystals exhibiting disordered carbonyl and chlorido ligands.[7]

Furthermore, the synthesis and the molecular structure of *trans*-[$RhCl_2$(P*i*Pr$_3$)$_2$] was described independently by two other groups.[8,9] *Harlow* and co-workers obtained this complex as a by-product during the reaction of **1** with P*i*Pr$_3$ in a nitrogen atmosphere. This Rh^{II} complex was finally obtained by the authors in a defined manner by the reaction of complex **1** with the phosphane in a nitrogen atmosphere using *N*-chlorosuccinimide (NCS) as the oxidizing agent. A second method started from *trans*-[$RhCl(N_2)$(P*i*Pr$_3$)$_2$] using the same oxidizing agent.[8] *Werner* et al. obtained *trans*-[$RhCl_2$(P*i*Pr$_3$)$_2$] during the reaction of [{Rh(μ-Cl)(P*i*Pr$_3$)$_2$}$_2$] with carbon tetrachloride.[9] In contrast to the former report,[8] in which the authors described this rhodium(II) species as dark red crystals, *Werner* and co-workers reported this complex as deep blue crystals.

Presumably, there is a possible explanation, why the latter discrepancies concerning the colors of the same compound were reported. In this context *Bennett* and *Longstaff* described, already in 1969, that *trans*-[$RhCl_2${P(*o*-tolyl)$_3$}$_2$] crystallized as a solid in two modifications.[10] They reported a blue-green paramagnetic modification from ethanol at room temperature and a purple paramagnetic modification, which was obtained at 273 K from dichloromethane. Moreover, they described a possible transformation of both modifications into each other. For example, by dissolving the purple solid in acetone at room temperature they obtained the blue-green modification. Unfortunately, no X-ray crystal structure data of both these modifications have been reported to date.

Results and Discussion

To obtain compound **2** by a more defined method in higher yields we checked the above-mentioned procedure.[8] Thus we reacted **1** with *t*Bu_2PPh (molar ratio Rh:P of 1:2) in THF at room temperature using *N*-chlorosuccinimide as the oxidizing agent. During 2 h a dark red-brown solution resulted, which precipitated **2** as greenish-blue powder. The solid was washed with diethyl ether and dried in vacuo. Crystallization from hot THF afforded finally the product in 39 % yield as well-shaped dark red crystals suitable for X-ray diffraction. Thus **2** crystallized from THF as crystals belonging to the orthorhombic space group *Pbca* with four molecules in the unit cell. A view of the molecular structure of **2** in the crystal is shown in Figure 1; selected bond lengths and angles are given in the figure caption. The coordination sphere around the rhodium atom can be described as nearly square planar with the bulky phosphane ligands in *trans* position to each other. The molecule **2** lies on a crystallographic inversion center. The same was reported for the closely related compound *trans*-[$RhCl_2$(P*i*Pr$_3$)$_2$].[8,9] Moreover, the results of the crystal and molecular structure determination of **2** are in good agreement with the reported ones of the related complex *trans*-[$PdCl_2$(*t*Bu_2PPh)$_2$].[11] Even the latter compound crystallized in the orthorhombic space group *Pbca* with very similar unit-cell parameters, confirming that crystals of **2** and the palladium species are isomorphous.

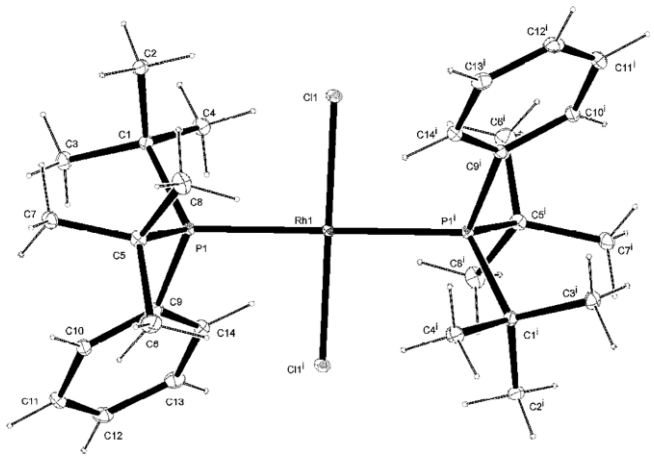

Figure 1. Molecular structure of **2** in the crystal (ORTEP drawing and atom labeling scheme with 50 % probability level). Selected bond lengths /Å and angles /°: Rh1–Cl1, 2.3094(7); Rh1–P1, 2.4074(7); P1–C1, 1.9062(15); P1–C5, 1.8979(16); P1–C9, 1.8389(15); C1–C2, 1.541(2); C5–C6, 1.544(2); C9–C10, 1.3994(19); C9–C14, 1.400(2). Cl1–Rh1–P1, 92.35(1); Cl1–Rh1–Cl1^i, 180.00; Cl1–Rh1–P1^i, 87.65(1); P1–Rh1–P1^i, 180.00; Rh1–P1–C1, 117.86(4); Rh1–P1–C5, 107.90(5); Rh1–P1–C9, 112.58(5); C1–P1–C5, 110.48(6); C1–P1–C9, 99.17(6), C5–P1–C9, 108.39(6).

The collection of NMR spectroscopic data of **2** in solution was complicated by the following reasons. Although **2** was stable as solid, even under air conditions for months (!), this could not be confirmed during dissolution of the solid in organic solvents. Here the deep red crystals showed the peculiarity to afford no corresponding red solutions. Contrary these solutions appeared immediately rather orange or yellow. The ^{1}H NMR (400 MHz) spectrum of **2** in CD_2Cl_2 showed two very broad signals at δ = 9.06 and 6.42 ppm that were obviously caused by the expected paramagnetism of the title compound **2**. However, beside the latter ones, well-resolved signals could also be observed. A doublet at δ = 1.20 ppm ($^3J_{PH}$ = 11.6 Hz) and two multiplets at 7.70 and 7.36 could be assigned to the free ligand *t*Bu_2PPh. This assumption was unambiguously further confirmed by the $^{31}P\{^1H\}$ NMR spectrum (CD_2Cl_2) showing a singlet at δ = 39.9 ppm indicating the free *t*Bu_2PPh.

In contrast to the ^{1}H NMR spectrum, the $^{31}P\{^1H\}$ NMR spectrum of **2** exhibited only sharp signals not hinting at a paramagnetic component in the solution. Here two main species were detected at 39.9 (s) and 62.6 ppm (d, J_{RhP} = 99.4 Hz). The singlet was assigned to the free ligand *t*Bu_2PPh as mentioned before. The observed doublet indicated a species containing a direct Rh–P bond caused by the coupling with the rhodium nucleus. Interpreting these observations we assumed in solution an equilibrium between complex **2**, a dinuclear Rh^{II} species, [{Rh(μ-Cl)Cl(*t*Bu_2PPh)}$_2$] (**3**), and the free ligand *t*Bu_2PPh. The hypothetical compound **3** may contain a Rh–Rh bond, therefore the paramagnetism should be compensated resulting in the well-resolved NMR signal.

The lack of a signal in the $^{31}P\{^{1}H\}$ NMR spectrum indicating the paramagnetic species **2** seemed unclear. It could be reasonable that the signal corresponding to the mononuclear title complex disappeared in the background of the spectrum because of shortened relaxation processes. Many attempts to separate the three discussed species from the solution equilibrium to obtain **3** as crystals for an X-ray diffraction study failed till now. Our assumption that the equilibrium scenario should be realistic was manifested mainly by the fact that, on cooling, these solutions afforded red crystals of **2** again by crystallization. That means that a reaction behavior in light of disproportionation processes, which has been often discussed for such systems in the literature,[2] could be ruled out with certainty. The solid-state ^{31}P NMR spectrum (202 MHz) of **2** showed only one broad signal centered at δ = 54.4 ppm and indicated, not so clearly, the paramagnetism of this species. However, the paramagnetism of **2** was unambiguously confirmed by ESR spectroscopic measurements. The ESR powder spectrum of **2** at room temperature and at 77 K, respectively, showed various signals and provided evidence for the oxidation state +II (d^7, one unpaired electron) in the title complex (see Figure S1, Supporting Information). The shapes of the spectra were in good accordance with the reported ones for the closely related compounds $[RhCl_2(PR_3)_2]$ (*R* = cyclohexyl, *o*-tolyl).[12] The spectra were temperature dependent. Unfortunately, no crystal data of the latter species for comparison purposes were available to date.

Figure 2 shows the UV/Vis spectrum of **2** in a diffuse-reflectance setup. The same spectra were obtained for a blue powder of **2** as well as ground red crystals from recrystallization batches. The ordinate is assigned to the Kubelka–Munk function, the entire curve was deconvolved by seven Gauss functions. The four most intense bands are listed in Table 1.

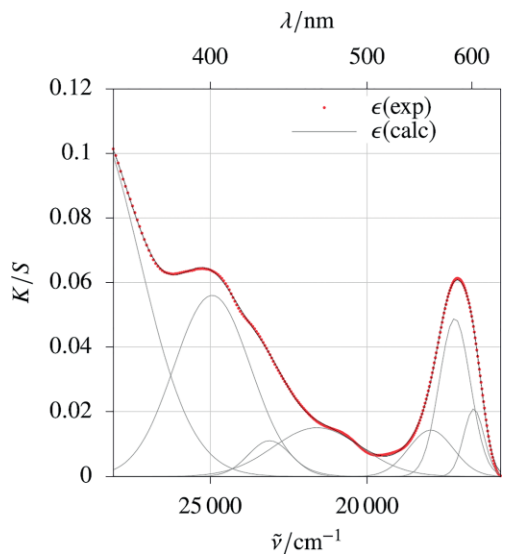

Figure 2. The Kubelka–Munk function *K*/*S* vs. the wave number for a solid sample of **2**, diluted with barium sulfate. Positions of the maxima: $\tilde{\nu}$ = 28943, 24935, 23105, 21591, 17968, 17205, 16599 cm^{-1}; λ in the same order: 346, 401, 433, 463, 557, 581, 602 nm.

Table 1. The positions of the four most intense, LMCT-type maxima of **2**.

$\tilde{\nu}$ /cm^{-1}	TDDFT
17205	15630
21591	21053
24935	23759
28943	26542

The distinct absorption around 580 nm is responsible for the blue color. The entire spectrum in the visible range should result in a purple color.

Computational Analysis of the Ground and Excites States of 2

Calculations within the framework of density-functional theory as well as preliminary calculations with wave-function methods are dominated by a small energetic difference of the molecular orbitals with Rh-d(z^2) and Rh-d(xz) contribution (axes: z normal to the RhP_2Cl_2 plane, x close to the Rh–Cl axis). All four ligands combine with d(z^2) to a σ-antibonding MO, whereas the chlorido ligands form π-antibonds with d(xz). Already in 1977, *van Gaal* et al. formulated a mixed d(z^2)/d(xz) occupation in their attempts to model ESR experiments on the blue compound $[RhCl_2(PCy_3)_2]$.[12] In a later work, *Harlow* et al. stressed the partial occupancy, instead of a full electron pair of the Rh-d(xz)/Cl-p(z) antibonds, as the origin of an unexpectedly short Rh–Cl bond (2.298 Å, compare 2.366 Å for Rh–P) in the related compound $[RhCl_2(PiPr_3)_2]$.[8] A routine DFT approach on the BP86/def2-TZVP level of theory, including Grimme's D3 van der Waals correction, confirmed the X-ray analysis within generally acceptable deviations of atomic distances and bond angles (Table 2). At this level, the singly occupied MO (SOMO) was the d(xz)-based orbital, thus leaving d(z^2) fully occupied. Accordingly, a closer look at the calculated distances revealed them to be a bit short. In order to lift the strict assignment of a $d(z^2)^2d(xy)^1$ configuration, we performed a series of computations.

Table 2. Distances /Å and angles /° for **2**. DFT calculations on the BP86/def2-TZVP level of theory. GS: ground state; root 1: first excited state in a TDDFT approach; 5000 K: temperature used for Fermi smearing in a finite-temperature DFT calculation.

	Rh–Cl	Rh–P	P–Rh–Cl
X-ray	2.3094(7)	2.4074(7)	92.35(1)
DFT (GS)	2.295	2.384	92.15
DFT (root 1)	2.339	2.382	92.90
DFT (GS, 5000 K)	2.323	2.450	92.32

(1) A TDDFT calculation on the TPSSh/def2-TZVP level revealed the $d(z^2)^1d(xy)^2$ configuration as the first excited state ("root 1"), about 4000 cm^{-1} above the ground state. Geometry optimization (BP86/def2-TZVP, D3) of the excited-state configuration showed, in agreement with *Harlow's* considerations,[8] a longer Rh–Cl bond together with an almost unaltered Rh–P distance (Table 2).

(2) As an entry to a correlated treatment, Grimme's fractional-occupation-number-weighted density (FOD) was calcu-

lated.[13] As a result, the molecular orbitals with Rh-d contributions showed marked static correlation in terms of their FOD values. Specifically, FODs decreased in the order d(xz) > d(z^2) > d(xy) on the TPSS/def2-TZVP level, and d(z^2) > d(xz) > d(xy) on the BHLYP/def2-TZVP level (both methods were employed using the recommended smearing temperatures, 5000 K and 15000 K, respectively). In addition to the calculation of FODs with the BP86/def2-TZVP-ground-state geometry, the structural parameters were optimized in a finite-temperature approach on the TPSS/def2-TZVP level of theory (Table 2).

(3) Attempts to use the CASSCF method next were impeded by both the size of the entity in question and rotations of metal orbitals to pure ligand MOs in the course of preliminary calculations. Since multideterminental methods appear as adequate in terms of the FOD analysis, we thus switched to a truncated hypothetical model compound with two trimethylphosphane ligands instead of the bis(*tert*-butyl)phenylphosphane ligands of **2** at this point (MOs of this model complex see Figure S2, Supporting Information, and cartesian coordinates from a BP86/def2-TZVP optimization see Tables, Supporting Information).

(4) The truncation of the bulky phosphane ligands in **2** to trimethylphosphane appears to be a rather conservative step in terms of the Rh–Cl distance (2.296 Å) and the P–Rh–Cl angles (92.5° for the obtuse angle) on the BP86/def2-TZVP(+D3) level. The distance from the central rhodium atom to the phosphorus atom of the smaller model phosphane decreases to 2.317 Å. The single spin resides in a d(z^2)/d(xz) linear combination. Starting from this structure, single-point CASSCF calculations converged in a small (7,5) active space (7 electrons in 5 orbitals). The extension to a second shell for rhodium converged as well CASSCF(7,10). Inclusion of dynamic correlation in a subsequent NEVPT2 step succeeded. However, the search for excitations results in only few low-lying excited states, which mirrored the multiconfigurational character of the system, and excitations to the far UV. In other words, the substance appeared to be colorless at this point. This situation changed after inclusion of the next occupied molecular orbital to a (9,11) active space. The additional MO was a Rh–P σ-bond with largely ligand and minor Rh-p_y character. Attempts to further enlarging the active space failed due to convergence problems with the practically inactive additional orbitals. The multiconfigurational character of the species is mirrored in the d orbital population. Thus, Löwdin reduced active MOs are populated by 1.95, 1.59, 1.57, 1.55, 1.55, 0.76 electrons in the order: Rh–P σ-bond, Rh-d-yz, xy, z^2, xz, x^2–y^2. These values result in Mulliken spin densities of the MOs with mainly Rh-d contribution 0.15, 0.14, 0.14, 0.14, 0.21 for the same order (Rh total: 0.77). In terms of configurations, the ground state is a mixture of two states of almost the same energy, the one with Rh-d(z^2) as the singly occupied orbital, the other with d(xz) singly occupied. The (9,11) calculation shows severe dynamical correlation. In the initial CASSCF calculation, the species remains colorless. However, a subsequent NEVPT2 step (including Orca's "canonstep 3" orbital relaxation option) revealed a single strong transition in the visible region (19336 cm^{-1}, 517 nm). In the excited state, an electron is transferred from the Rh–P σ-bond to the d subshell to fill the xz/z^2 hole. With this assignment, the interpretation of a TDDFT calculation was straightforward. At the TPSSh/def2-TZVP level of theory, the Rh–P-σ-bond-to-xz/z^2 transition appeared at 17078 cm^{-1} (586 nm).

(5) For **2**, the same transition was found at lower energy (first entry in Table 1). With this fixed point, other TDDFT transitions were assigned with the result that all of these resemble excitations from low-lying MOs with mainly ligand character to the β-LUMO. Hence, the color of **2** is a result of LMCT processes instead of d–d transitions within the open d subshell. It should be noted eventually, that the ESR analysis by *van Gaal* et al.[12] of a mixed d(xy)/d(z^2) occupation with three electrons was fully substantiated in the course of the various calculations.

Conclusions

A new representative of the rare class of mononuclear paramagnetic rhodium(II) complexes, *trans*-[$RhCl_2(tBu_2PPh)_2$] (**2**), was synthesized and characterized in a combined experimental and computational approach. The structure was determined by means of single-crystal X-ray diffractometry. Despite the fact that an unpaired electron resides on the central rhodium atom, no Rh–Rh bonds were found. Instead, mononuclear, low-spin-d^7 doublet central rhodium atoms were coordinated square-planarly by two *trans*-chlorido and two phosphane ligands. Distances and angles were reproduced at an appropriate level of accuracy in a DFT calculation.

In addition, a wave-function-theory-based (WFT) treatment on a correlated level was performed on a truncated model complex. As a result, the ground state of **2**, as has been recognized decades ago in the course of EPR measurements, is multiconfigurational and, thus, is adequately described by a CASSCF(9,11) calculation with a subsequent NEVPT2 approach. The introduction of dynamic correlation in the latter step revealed necessary for the assignment of a typical electronic excitation in the visible region. Based on the WFT analysis, more transitions in a TDDFT calculation were assigned. In fact, all the transitions were of the LMCT type. They all start in ligand-based MOs and end in the complex's β-LUMO, the Rh-d(xz)/(z^2) orbital. In solutions of **2**, the NMR spectroscopic results indicated a dynamic equilibrium between **2**, a hypothetical dinuclear Rh^{II} species [{Rh(μ-Cl)-Cl(tBu_2PPh)}$_2$], and the free ligand tBu_2PPh. Attempts to isolate the tentative dinuclear species from the solution were unsuccessful so far. Efforts in this direction will be the subject of our future work.

Experimental Section

General: All preparative work was carried out in a dry nitrogen atmosphere using standard Schlenk techniques. Chemicals were purchased from Sigma/Aldrich and used as received. [{Rh(μ-Cl)(coe)$_2$}$_2$] was prepared according to the literature procedure.[14] NMR spectra were recorded with a Jeol Eclipse 400 instrument operating at 400 MHz (^{1}H) and at 162 MHz (^{31}P). Chemical shifts are given in ppm relative to TMS (^{1}H) and 85 % H_3PO_4 (^{31}P). ^{31}P NMR MAS spectra were

recorded with a Bruker Avance-III 500 spectrometer using a Larmor frequency of $\nu_0(^{31}P)$ = 202.5 MHz. For the measurements a commercial 2.5 mm MAS probe was used. UV/Vis spectra were recorded with a Varian Cary 50 spectrometer. The ESR spectra were acquired with a Bruker EMX-Nano X-band EPR instrument. Elemental analyses were performed by the Microanalytical Laboratory of the Department of Chemistry, LMU Munich, using a Heraeus Elementar Vario EL instrument.

Orca4 was used for all computations.[15] The methods as well as the basisi set def2-TZVP were used as integrated in Orca. In the DFT part, Grimmes's D3 van der Waals correction was applied,[16] but no solvent model was used.

Synthesis of *trans*-[RhCl$_2$(*t*Bu$_2$PPh)$_2$] (2): To a solution of **1** (180 mg, 0.25 mmol) in THF (5 mL) *t*Bu$_2$PPh (0.24 mL, 1 mmol) was added at room temperature with stirring. After 10 min *N*-chlorosuccinimide (70 mg, 0.5 mmol) was added and the solution stirred at room temperature for 2 h. During this time the color of the solution changed from orange to dark red-brown and a green-blue powder precipitated. The powder was filtered off and washed twice with diethyl ether (10 mL) and dried in vacuo. The product was recrystallized from 10 mL of hot THF. Standing overnight at room temperature afforded well-shaped dark red crystals suitable for X-ray diffraction. Yield: 120 mg (39 %). $C_{28}H_{46}Cl_2P_2Rh$ (618.43): C 54.15 (calcd. 54.38); H 7.35 (7.50), Cl 11.19 (11.47) %. **^{1}H NMR** (CD_2Cl_2, 20 °C): δ = 9.06 (br), 6.42 (br). **^{31}P{^{1}H} NMR** (CD_2Cl_2, 20 °C): δ = 62.6 (d, J_{RhP} = 99.4, presumably [{Rh(μ-Cl)Cl(*t*Bu$_2$PPh)}$_2$], 39.9 (s, *t*Bu$_2$PPh). **^{31}P{^{1}H} NMR MAS** (solid, 202.5 MHz, 20 °C): δ = 54.4 (br) ppm. **UV/Vis** (CH_2Cl_2): 571 nm. **UV/Vis** (solid): 581 nm.

Crystal Structure Determination and Refinement: Crystals of **2** suitable for X-ray diffraction were obtained from hot THF by cooling to room temperature and standing overnight. Crystals were selected by means of a polarization microscope, mounted on the tip of a glass fiber, and investigated with a Bruker D8 venture TXS diffractometer using graphite-monochromated Mo-K_α radiation (λ = 0.71073 Å). The structure was solved by direct methods (SIR97)[17] and refined by full-matrix least-squares calculations on F^2 (SHELXL-97).[18] Anisotropic displacement parameters were refined for all non-hydrogen atoms. Details of the crystal data, data collection, structure solution, and refinement parameters of compound **2** are summarized in Table 3.

Table 3. Details of the crystal structure determination of **2**.

	$C_{28}H_{46}Cl_2P_2Rh$
T /K	100(2)
Crystal system	orthorhombic
Space group	*Pbca*
a /Å	10.891(2)
b /Å	16.288(4)
c /Å	16.586(3)
V /Å^3	2922.8(11)
Z	4
Density /g·cm^{-3}	1.405
μ /mm^{-1}	0.892
θ range /°	3.338–26.39
Reflections, collected	74673
Reflections, independent	2967
R_{int}	0.0370
wR_2 (all data)	0.0476
R_1	0.0189
S	1.097
$\Delta\rho_{fin}$ (max/min) /e·Å^{-3}	0.326 / –0.438

Crystallographic data (excluding structure factors) for the structure in this paper have been deposited with the Cambridge Crystallographic Data Centre, CCDC, 12 Union Road, Cambridge CB21EZ, UK. Copies of the data can be obtained free of charge on quoting the depository number CCDC-1826238 (**2**) (Fax: +44-1223-336-033, E-Mail: deposit@ccdc.cam.ac.uk, http://www.ccdc.cam.ac.uk).

Supporting Information (see footnote on the first page of this article): ESR spectra and details of computational analysis.

Acknowledgements

The Department of Chemistry of the Ludwig-Maximilians-Universität Munich is gratefully acknowledged for financial support of these investigations. *L. Daumann* is thanked for recording the ESR spectra. *Johnson Matthey* plc, Reading, UK, is gratefully acknowledged for a generous loan of hydrated rhodium(III) chloride.

Keywords: Crystal structure; DFT calculations; Phosphane complexes; Rhodium

References

[1] H.-C. Böttcher, P. Mayer, *Z. Naturforsch. B* **2008**, *63*, 1035.
[2] D. G. DeWit, *Coord. Chem. Rev.* **1996**, *147*, 209.
[3] K. Fuchigami, N. P. Rath, L. M. Mirica, *Inorg. Chem.* **2017**, *56*, 9404 and references cited therein.
[4] D. L. Thorn, T. H. Tulip, J. A. Ibers, *J. Chem. Soc., Dalton Trans.* **1979**, 2022.
[5] C. Busetto, A. D′Álfonso, F. Maspero, G. Perego, A. Zazzetta, *J. Chem. Soc., Dalton Trans.* **1977**, 1828.
[6] C. A. Ogle, T. C. Masterman, J. L. Hubbard, *J. Chem. Soc., Chem. Commun.* **1990**, 1733.
[7] K. R. Dunbar, S. C. Haefner, *Inorg. Chem.* **1992**, *31*, 3676.
[8] R. L. Harlow, D. L. Thorn, R. T. Baker, N. L. Jones, *Inorg. Chem.* **1992**, *31*, 993.
[9] T. Rappert, J. Wolf, M. Schulz, H. Werner, *Chem. Ber.* **1992**, *125*, 839.
[10] M. A. Bennett, P. A. Longstaff, *J. Am. Chem. Soc.* **1969**, *91*, 6266.
[11] C. M. DiMeglio, L. A. Luck, C. D. Rithner, A. L. Rheingold, W. L. Elcesser, J. L. Hubbard, C. H. Bushweller, *J. Phys. Chem.* **1990**, *94*, 6255.
[12] H. L. M. Van Gaal, J. M. J. Verlaak, T. Posno, *Inorg. Chim. Acta* **1977**, *23*, 43.
[13] a) S. Grimme, A. Hansen, *Angew. Chem.* **2015**, *127*, 12483; b) C. A. Bauer, A. Hansen, S. Grimme, *Chem. Eur. J.* **2017**, *23*, 6150.
[14] A. van der Ent, A. L. Onderdelinden, *Inorg. Synth.* **1990**, *28*, 90.
[15] F. Neese, *Wiley Interdisciplinary Reviews: Computational Molecular Science* **2012**, *2*, p. 73.
[16] S. Grimme, J. Antony, S. Ehrlich, H. Krieg, *J. Chem. Phys.* **2010**, *132*, 154104.
[17] A. Altomare, M. C. Burla, M. Camalli, G. L. Cascarano, C. Giacovazzo, A. Guagliardi, A. G. G. Moliterni, G. Polidori, R. Spagna, *J. Appl. Crystallogr.* **1999**, *32*, 115.
[18] G. M. Sheldrick, *Acta Crystallogr., Sect. A* **2008**, *64*, 112.

Received: July 6, 2018
Published online: September 25, 2018

